Volume 22
Number 26
14 July 2020
Pages 4341–4502

CrystEngComm

rsc.li/crystengcomm

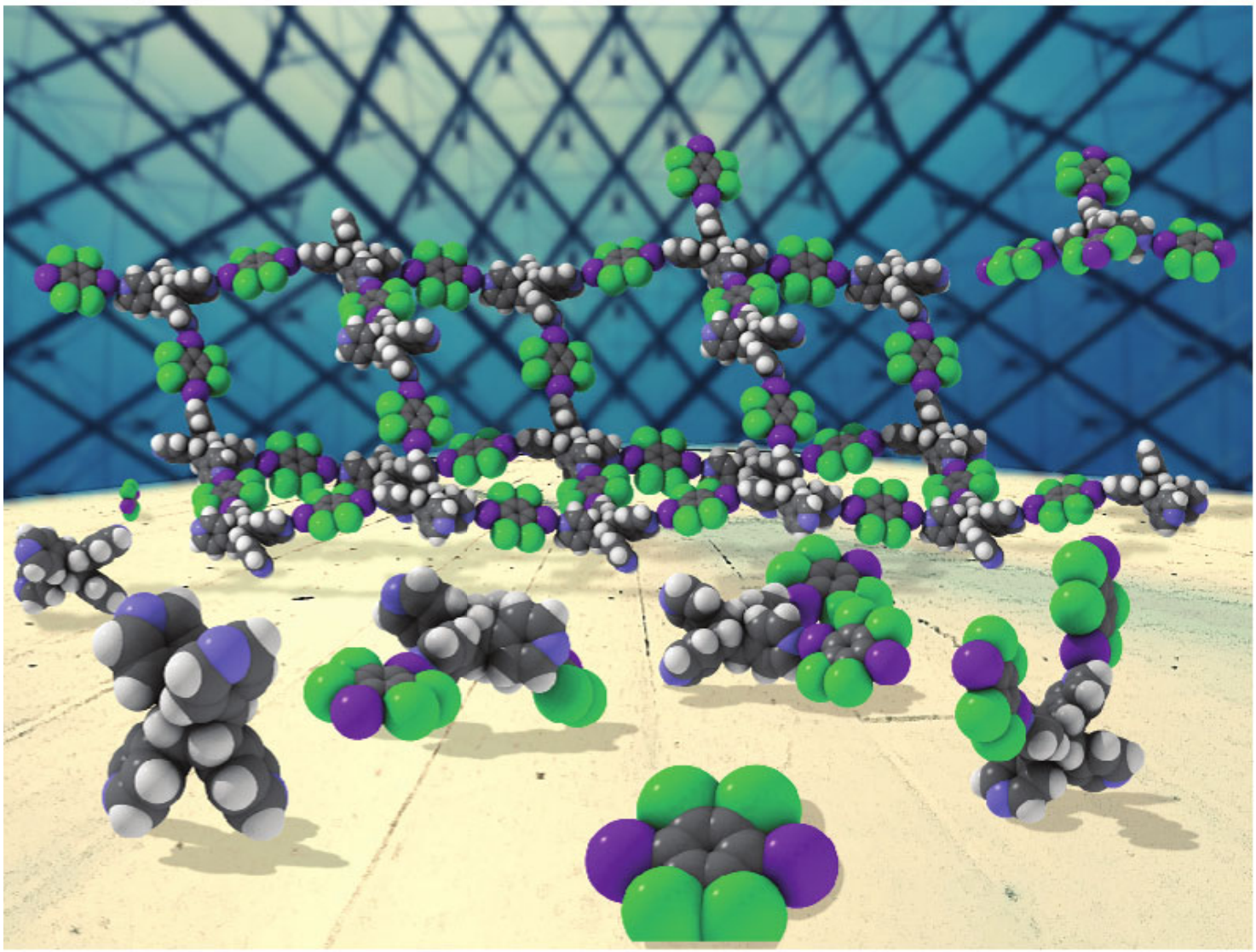

ISSN 1466-8033

ROYAL SOCIETY OF CHEMISTRY

COMMUNICATION

Ryan H. Groeneman *et al.*

A diamondoid net sustained by halogen bonds: employing a cyclobutane to generate a tetrahedral architecture

CrystEngComm

ROYAL SOCIETY OF CHEMISTRY

COMMUNICATION

View Article Online
View Journal | View Issue

Cite this: *CrystEngComm*, 2020, **22**, 4349

Received 26th April 2020,
Accepted 14th May 2020

DOI: 10.1039/d0ce00627k

rsc.li/crystengcomm

A diamondoid net sustained by halogen bonds: employing a cyclobutane to generate a tetrahedral architecture†

Shalisa M. Oburn, [a] Carlos L. Santana,[b] Elizabeth Elacqua [a] and Ryan H. Groeneman *[b]

A halogen-bonded eight-fold interpenetrated diamondoid net was constructed employing a node generated in the solid state. Specifically, co-crystallization of a tetrahedral-like tecton, *rctt*-tetrakis(4-pyridyl)cyclobutane (4,4′-TPCB), combined with a rigid halogen-bond donor, 1,4-diiodoperchlorobenzene, achieved a diamondoid architecture. In the co-crystal, 4,4′-TPCB is found to form three types of linkages based on one *cis*- and two *trans*-orientations enabled by the intrinsic *rctt*-stereochemisty of the central cyclobutane ring. Thus, 4,4′-TPCB is able to adapt to the constraints of the diamondoid net owing to the flexibility of the pendant 4-pyridyl groups.

Predictability and reliability in the formation of multi-component solids still remains a fundamental goal in the design of highly-connected networks.[1–3] Therefore, when designing these multi-component nets, careful consideration of both the node and the linker is required, since each will ultimately influence the overall connectivity as well as the resulting topology.[4] Successful approaches in forming these targeted architectures have included diversifying bonding capabilities[5,6] and bond angle flexibility[7] which allows the various components to assemble in the solid state. This tolerance allows these molecules/ions to interact even with slight misalignment of the donor and acceptor sites.

Tectons generated in the solid state, such as through the [2+2] cycloaddition reaction,[8] have been successfully incorporated into these connected networks. In particular, the photoproduct *rctt*-tetrakis(4-pyridyl)cyclobutane (**4,4′-TPCB**) has been utilized as a tetrahedral-like connecting node in various extended solids.[9–17] This cyclobutane node contains four identical and divergent pendant groups radially splayed from the central cyclobutane ring. Collectively, the 4-pyridyl groups can act as a 4-connecting node, forming coordinated covalent bonds with different metal centres as well as participating in various halogen and hydrogen bonds. Previously, Metrangolo and Resnati reported the ability of **4,4′-TPCB** to yield a two-fold interpenetrated two-dimensional square lattice (**sql**) net when coupled with the halogen-bond donor 1,4-diiodoperfluorobenzene ($C_6I_2F_4$).[10]

A highly studied architecture within these polymeric solids has been the diamondoid (**dia**) network which is a three-dimensional solid containing a tetrahedral node.[18–21] Recently, Aakeröy and co-workers utilized tetrakis(4-(iodoethynyl)phenyl)methane as a halogen-bond donor that adopts the required tetrahedral geometry due to the central sp^3-hybridized carbon.[22] The extended solid forms *via* I···X$^-$ halogen bonds with various co-formers based upon tetraphenylphosphonium halides.

Recently, the ability of 1,4-diiodoperchlorobenzene ($C_6I_2Cl_4$) to act as a halogen-bond donor has been reported.[23–25] Similar to $C_6I_2F_4$, molecules of $C_6I_2Cl_4$ form reliable I···N halogen bonds to pyridyl groups and as a result should be a suitable linker in the formation of extended solids. As such, it was envisioned that a purely organic net incorporating **4,4′-TPCB** could be realized when combined with $C_6I_2Cl_4$.[7]

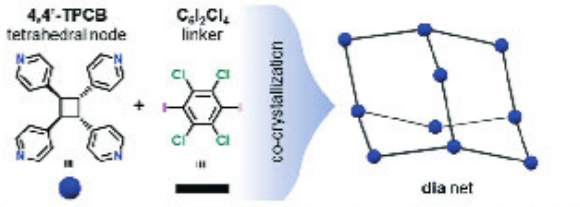

Scheme 1 Components of the **dia** net topology where the tetrahedral node was generated from a solid-state [2+2] cycloaddition reaction.

[a] *Department of Chemistry, The Pennsylvania State University, University Park, PA, 16802, USA*
[b] *Department of Biological Sciences, Webster University, St. Louis, MO 63119, USA. E-mail: ryangroeneman19@webster.edu; Tel: +1 314 246 7466*

† Electronic supplementary information (ESI) available: Experimental details, single crystal X-ray data, and TOPOS report. CCDC 1996696. For ESI and crystallographic data in CIF or other electronic format see DOI: 10.1039/d0ce00627k

Using this as inspiration, we report the first fully-organic **dia** net based upon **4,4′-TPCB** as a 4-connecting node sustained by I···N halogen bonds and subsequent formation of an eight-fold interpenetrated solid (Scheme 1). A rigid halogen-bonding linker $C_6I_2Cl_4$ was combined with **4,4′-TPCB** to generate a co-crystal in the form of (**4,4′-TPCB**)·2($C_6I_2Cl_4$)·2(**toluene**) (**1**). The ability of **4,4′-TPCB** to yield different topologies is attributed to the flexibility of the 4-pyridyl groups to adopt and conform to the constraints of the **dia** topology.

The components of this **dia** net are not commercially available and thus, required synthesis. The linker $C_6I_2Cl_4$ was synthesized using a previously reported method.[26] In addition, the node **4,4′-TPCB** was generated through a template-based approach utilizing resorcinol;[27] after quantitative photoreaction, resorcinol was removed using base extraction.

The co-crystal **1** was realized by combining a warm ethanol solution of **4,4′-TPCB** and a toluene solution of $C_6I_2Cl_4$ (respective 1 : 2 molar ratio) that was then allowed to cool and slowly evaporate. Colourless block-like single crystals suitable for X-ray diffraction formed within 2 days.

Diffraction data determined the formula of **1** to be (**4,4′-TPCB**)·2($C_6I_2Cl_4$)·2(**toluene**). The components of the solid crystallize in the orthorhombic space group *Aba*2. The asymmetric unit contains half of a molecule of **4,4′-TPCB**, one molecule of $C_6I_2Cl_4$, and two disordered toluene molecules with half occupancies due to mirror plane symmetry (Fig. S1†). The 4-pyridyl groups on **4,4′-TPCB** all participate in I···N halogen bonds with $C_6I_2Cl_4$ [I···N 2.841(3) and 2.872(3) Å; C–I···N 175.4(1) and 177.2(1)°] (Fig. 1).

A notable feature of **1** is its ability to assemble into a three-dimensional halogen-bonded uninodal **dia** net (point symbol 6^6) as determined by TOPOS.[28] Nodes of the **dia** net are defined by **4,4′-TPCB**, with centroids near the centre of the cyclobutane rings. The expected and observed *rctt*-stereochemistry[27] of the cyclobutane core provides tetrahedrally-disposed *cisoid* and *transoid* halogen-bond-acceptor sites to sustain the 4-connected net (Fig. 1). The ability of **4,4′-TPCB** to adapt to diverse topologies based on the identity of the linker is highlighted by the flexibility of the pendant 4-pyridyl groups. In contrast, the rigidity of the *rctt*-conformation around the cyclobutane ring, generated through covalent bond formation *via* the [2+2] cycloaddition reaction, mitigates other undesirable motifs constructed from this tetrahedral node.

Molecules of **4,4′-TPCB** and $C_6I_2Cl_4$ halogen bond to generate six-membered rings that are interconnected, which is a requirement of the **dia** net (Fig. 2a and 3). As a result of **dia** net formation, the co-crystal generates hexagonal channels running throughout the structure (Fig. 2b). Due to the size of these channels, the large void space is addressed by interpenetration of seven additional independent **dia** nets resulting in a remarkable overall eight-fold interpenetrated structure (Fig. 2c).

Complexity within the **dia** net arises based upon the connectivity generated though the stereochemistry of the 4-pyridyl groups disposed around the cyclobutane core. Every node supports three types of linkages based on positions and relative orientations of the 4-pyridyl groups around the cyclobutane ring, namely 1,2-*cis*, 1,3-*trans*, and 1,4-*trans* (Fig. 3). Six-membered rings characteristic of the **dia** topology are generated from two 1,2-*cis*, two 1,3-*trans*, and two 1,4-*trans* linkages in an alternating pattern. Due to these different stereochemical orientations in **4,4′-TPCB**, along with the divergent nature of the $C_6I_2Cl_4$ linker, the six-membered rings adopt a chair-like conformation with relatively large edge lengths of 43.97 Å × 22.68 Å (Fig. 3).

The connectivity of each cyclobutane to generate halogen-bonded six-membered rings differs from the previously reported four-membered rings of the **sql** net observed within (**4,4′-TPCB**)·2($C_6I_2F_4$) (Fig. 4).[10] Specifically in the **sql** net, the corners of the smallest four-membered rings are based upon molecules of **4,4′-TPCB** interacting though halogen bonds with $C_6I_2F_4$ *via* 1,2-*cis* and 1,3-*trans* orientations of **4,4′-TPCB** (Fig. 4). The 1,4-*trans* orientation serves to connect edges of two 4-membered rings within the **sql** net, rather than forming the required six-membered rings of the **dia** net.

Within (**4,4′-TPCB**)·2($C_6I_2F_4$), molecules of $C_6I_2F_4$ are found to engage in both homogenous face-to-face π-π stacking as well as heterogeneous π–π interactions with 4-pyridyl rings of

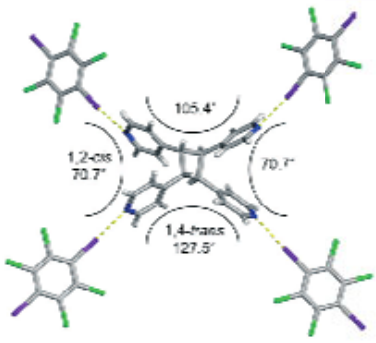

Fig. 1 X-ray structure of **1** illustrating the 4-connected **4,4′-TPCB** node halogen bonding to four $C_6I_2Cl_4$ linkers.

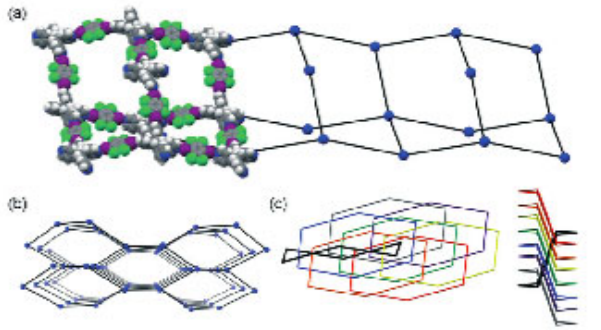

Fig. 2 Topology of **1**: (a) X-ray structure with a space-filling view of molecular building blocks constructing a single **dia** net, (b) illustration of the extended hexagonal channels, and (c) eight-fold interpenetrated **dia** nets highlighted in different colours.

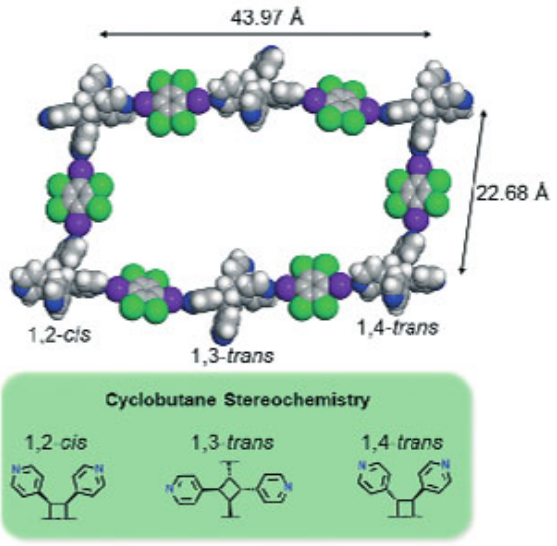

Fig. 3 X-ray structure of **1** illustrating the six-membered ring generated from the three unique linkages, namely 1,2-*cis*, 1,3-*trans*, and 1,4-*trans*.

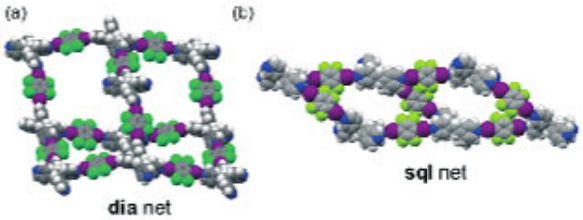

Fig. 4 Space-filling view of the nets incorporating **4,4′-TPCB**: (a) **dia** net of **1** and (b) **sql** net of (**4,4′-TPCB**)·2($C_6I_2F_4$).

4,4′-TPCB. Alternatively, $C_6I_2Cl_4$ molecules within **1** are found to engage in homogenous face-to-face π–π interactions (centroid–centroid: 4.29 Å) as well as heterogeneous face-to-face π–π stacking with an included toluene molecule (centroid–centroid: 3.55 Å) (Fig. 5a). This π–π stacking arrangement generates an infinite column of AABAA type running along the crystallographic *a*-axis. A second unique toluene molecule participates in edge-to-face π–π (3.76 Å) and C–H···π (3.60 Å) interactions to **4,4′-TPCB** which results in a large obtuse angle (127.5°) for the 1,4-*trans* linkage (Fig. 1 and 5b). Additionally, a second edge-to-face π–π interaction occurs between **4,4′-TPCB** and $C_6I_2Cl_4$ through Cl···π interactions[29] (3.30 Å) which also generates an obtuse angle (105.4°) around the cyclobutane core (Fig. 1 and 5b).

Ultimately, the ability of **4,4′-TPCB** to adopt to both a nearly square-planar node in the **sql** net as well as a tetrahedral-like node in the **dia** net is attributed to the flexibility in the positioning of the 4-pyridyl groups (*i.e.* distances separating face-to-face 4-pyridyl rings). This is accentuated by a variation of bond angles between donor N-atoms of the 4-pyridyl groups in relation to the centre of

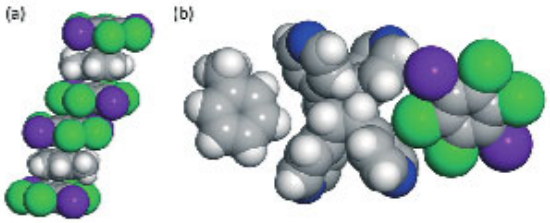

Fig. 5 X-ray structure of **1**: (a) π–π stacking arrangements of the aromatic rings and (b) edge-to-face π–π stacking interaction involving **4,4′-TPCB**. The disorder in toluene was removed for clarity.

the cyclobutane ring when compared to the **sql** net (Fig. S2†). Notable differences occur in 1,2-*cis* groups, where unidirectional 4-pyridyl groups staggered in a gauche orientation (**dia** = 29.8°, **sql** = 21.6° and 23.9°) are subject to steric repulsion[30] causing rings to 'pucker' out from the central cyclobutane ring (Fig. S3†). Specifically, the corresponding geometries observed between the 1,2-*cis* 4-pyridyl groups, (**dia** = 70.7°, **sql** = 59.1° and 67.3°) and a subsequent change in the 1,4-*trans* groups (**dia** = 127.5 and 105.4°, **sql** = 105.8 and 139.0°), allows for the formation of the **dia** net (Fig. 4). Lastly, tolerance in the C–I···N halogen-bond angles also plays a role in the formation of the given net. In particular, the **dia** net has nearly linear bond angles with values ranging between 175–177° while the **sql** net has much lower values ranging from 162–178°.

The stereoisomer *rtct*-**4,4′-TPCB** is considered a more suitable tetrahedral node in terms of the bond angle between pendant 4-pyridyl groups. In particular, Vittal and co-workers reported the formation of an extended network based upon *rtct*-**4,4′-TPCB** along with cobalt(II) fluoride that resulted in a nearly tetrahedral bond angle between the 4-pyridyl groups with a value of 105.6°.[31] Although, *rtct*-**4,4′-TPCB** inherently is a more tetrahedral-like geometry, we demonstrated here that the *rctt*-isomer can also produce the required tetrahedral node to yield the **dia** net (Fig. S4†). The ability of *rctt*-**4,4′-TPCB** to adopt to various positions for the pedant groups as well as a wide range of halogen-bond angles[32] again illustrates its capacity to conform to the requirements for a particular net and adaptability to the constraints of a given linker. This resulting variation in the networks generates complexity from simplicity in these extended solids containing **4,4′-TPCB**.

Conclusions

In this Communication, we report the formation of a purely organic uninodal three-dimensional halogen-bonded **dia** net of composition (**4,4′-TPCB**)·2($C_6I_2Cl_4$)·2(**toluene**). The **dia** net is constructed using a product generated in the solid state, namely **4,4′-TPCB**, which acts as a 4-connecting node along with a rigid halogen-bonding linker $C_6I_2Cl_4$. The solid exhibits remarkable eight-fold interpenetration due to the large dimension of the **dia** net caused by the divergent

organic linker. The inherent flexibility of **4,4′-TPCB** allows the node to adapt to the constraints of a **dia** topology.

Conflicts of interest

There are no conflicts to declare.

Acknowledgements

R. H. G. gratefully acknowledges financial support from Webster University in the form of various Faculty Research Grants. S. M. O. gratefully acknowledges the Eberly College of Science at The Pennsylvania State University for the Eberly Postdoctoral Fellowship. E. E. acknowledges financial support from The Pennsylvania State University. Funding from the National Science Foundation (MRI, CHE-1827756) for the purchase of the Bruker Venture Duo Photon-II diffractometer is also acknowledged. Lastly, the authors would like to thank Professor Eric Bosch from Missouri State University for the donation of $C_6I_2Cl_4$ used in this contribution.

Notes and references

1 I. Huskić, I. V. Pekov, S. V. Krivovichev and T. Friščić, *Sci. Adv.*, 2016, **2**, e1600621.
2 F. Nouar, J. F. Eubank, T. Bousquet, L. Wojtas, M. J. Zaworotko and M. Eddaoudi, *J. Am. Chem. Soc.*, 2008, **130**, 1833.
3 S. J. Lyle, P. J. Waller and O. M. Yaghi, *Trends Chem.*, 2019, **1**, 172.
4 H. Jiang, J. Jia, A. Shkurenko, Z. Chen, K. Adil, Y. Belmabkhout, L. J. Weselinski, A. H. Assen, D.-X. Xue, M. O'Keeffe and M. Eddaoudi, *J. Am. Chem. Soc.*, 2018, **140**, 8858.
5 R.-B. Lin, Y. He, P. Li, H. Wang, W. Zhou and B. Chen, *Chem. Soc. Rev.*, 2019, **48**, 1362.
6 M. R. Montney, S. Mallika Krishnan, N. M. Patel, R. M. Supkowski and R. L. LaDuca, *Cryst. Growth Des.*, 2007, **7**, 1145.
7 S. M. Oburn, M. A. Sinnwell, D. P. Ericson, E. W. Reinheimer, D. M. Proserpio, R. H. Groeneman and L. MacGillivray, *IUCrJ*, 2019, **6**, 1032.
8 G. M. J. Schmidt, *Pure Appl. Chem.*, 1971, **27**, 647.
9 A. J. Blake, N. R. Champness, S. S. M. Chung, W.-S. Li and M. Schröder, *Chem. Commun.*, 1997, 1675.
10 M. Baldrighi, P. Metrangolo, F. Meyer, T. Pilati, D. Proserpio, G. Resnati and G. Terraneo, *J. Fluorine Chem.*, 2010, **131**, 1218.
11 D.-X. Li, C.-Y. Ni, M.-M. Chen, M. Dai, W.-H. Zhang, W.-Y. Yan, H.-X. Qi, Z.-G. Ren and J.-P. Lang, *CrystEngComm*, 2014, **16**, 2158.
12 J. I. Poong, H. G. Koo, H. M. Park, S. P. Jang, Y. J. Lee, C. Kim, S.-J. Kim and Y. Kim, *Inorg. Chim. Acta*, 2011, **376**, 605–611.
13 G. S. Papaefstathiou and L. R. MacGillivray, *Angew. Chem., Int. Ed.*, 2002, **41**, 2070.
14 M. Dai, W.-Y. Yan, Z.-G. Ren, H.-F. Wang, W.-J. Gong, F.-L. Li, X. Zhao, H.-X. Li and J.-P. Lang, *CrystEngComm*, 2012, **14**, 6230.
15 M. H. Mir, L. L. Koh, G. K. Tan and J. J. Vittal, *Angew. Chem., Int. Ed.*, 2010, **49**, 390.
16 J. Yong Lee, S. Jin Hong, C. Kim and Y. Kim, *Dalton Trans.*, 2005, 3716.
17 M. Dai, T.-Y. Gu, X. Zhao, H.-X. Li and J.-P. Lang, *CrystEngComm*, 2015, **17**, 8345.
18 M. J. Zaworotko, *Chem. Soc. Rev.*, 1994, **23**, 283.
19 I. A. Baburin, V. A. Blatov, L. Carlucci, G. Ciani and D. M. Proserpio, *Cryst. Growth Des.*, 2008, **8**, 519.
20 O. Ermer, *J. Am. Chem. Soc.*, 1988, **110**, 3747.
21 D. K. Kumar, D. A. Jose, A. Das and P. Dastidar, *Inorg. Chem.*, 2005, **44**, 6933.
22 C. A. Gunawardana, M. Đaković and C. B. Aakeröy, *Chem. Commun.*, 2018, **54**, 607.
23 E. Bosch, S. J. Kruse, H. R. Krueger and R. H. Groeneman, *Cryst. Growth Des.*, 2019, **19**, 3092.
24 E. Bosch, S. J. Kruse, E. W. Reinheimer, N. P. Rath and R. H. Groeneman, *CrystEngComm*, 2019, **21**, 6671.
25 S. J. Kruse, E. Bosch, F. Brown and R. H. Groeneman, *Cryst. Growth Des.*, 2020, **20**, 1969.
26 C. M. Reddy, M. T. Kirchner, R. C. Gundakaram, K. A. Padmanabhan and G. R. Desiraju, *Chem. – Eur. J.*, 2006, **12**, 2222.
27 L. R. MacGillivray, J. L. Reid and J. A. Ripmeester, *J. Am. Chem. Soc.*, 2000, **122**, 7817.
28 V. A. Blatov, A. P. Shevchenko and D. M. Proserpio, *Cryst. Growth Des.*, 2014, **14**, 3576.
29 I. S. Youn, D. Y. Kim, W. J. Cho, J. M. L. Madridejos, H. M. Lee, M. Kołaski, J. Lee, C. Baig, S. K. Shin, M. Filatov and K. S. Kim, *J. Phys. Chem. A*, 2016, **120**, 9305.
30 E. V. Rybak-Akimova, A. Y. Nazarenko, L. Chen, P. W. Krieger, A. M. Herrera, V. V. Tarasov and P. D. Robinson, *Inorg. Chim. Acta*, 2001, **324**, 1.
31 A. M. P. Peedikakkal, C. S. Y. Peh, L. L. Koh and J. J. Vittal, *Inorg. Chem.*, 2010, **49**, 6775.
32 M. A. Sinnwell, J. N. Blad, L. R. Thomas and L. R. MacGillivray, *IUCrJ*, 2018, **5**, 491.

